



Title	Constructal blade shape in nanofluids
Author(s)	Bai, C; Wang, L
Citation	Nanoscale Research Letters, 2011, v. 6 n. 1, p. X1-7
Issued Date	2011
URL	http://hdl.handle.net/10722/145034
Rights	Bai and Wang; licensee Springer.

NANO EXPRESS

Open Access

Constructal blade shape in nanofluids

Chao Bai, Liqiu Wang*

Abstract

Blade configuration of nanofluids has been proven to perform much better than dispersed configuration for some heat conduction systems. The analytical analysis and numerical calculation are made for the cylinder-shaped and regular-rectangular-prism-shaped building blocks of the blade-configured heat conduction systems (using nanofluids as the heat conduction media) to find the optimal cross-sectional shape for the nanoparticle blade under the same composing materials, composition ratio, volumetric heat generation rate, and total building block volume. The regular-triangular-prism-shaped blade has been proven to perform better than all the other three kinds of blades, namely, the regular-rectangular-prism-shaped blade, the regular-hexagonal-prism-shaped blade, and the cylinder-shaped blade. Thus, the regular-triangular-prism-shaped blade is selected as the optimally shaped blade for the two kinds of building blocks that are considered in this study. It is also proven that the constructal cylinder-regular-triangular-prism building block performs better than the constructal regular-rectangular-prism-regular-triangular-prism building block.

Introduction

Nanofluids are mixtures of nanoparticles and base fluids, which have different thermal conductivities [1-5]. They were identified and proposed as a result of people's persistent pursuit for more and more efficient heat-transfer media. It should be noted that conventional heat transfer fluids have normally very low thermal conductivity, thus destroying much exergy during heat transport. At present, a great amount of attention is paid to studies on nanofluids, with the aim of addressing many unsolved issues [6-10].

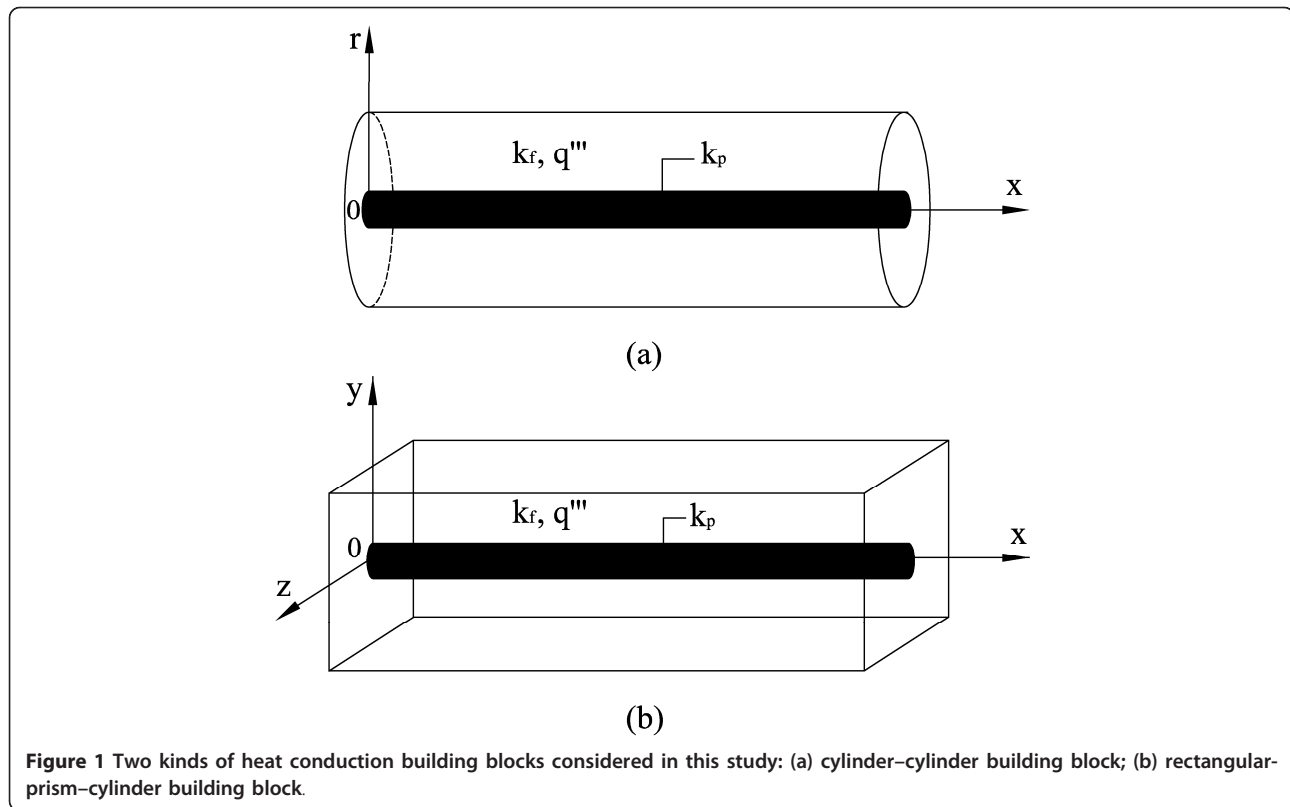
Constructal theory is a novel thought for nature and society [11-17]. It tries to explain phenomena based on optimization, or natural selection in biological terms. One of its viewpoints is that two flow mechanisms are better than one [18]. This is what one sees naturally in river basins, lung structure, and the percolation threshold effect [19]. Our previous studies have proved that the blade configuration of nanofluids is much better than the dispersed configuration for the two kinds of disk-shaped heat conduction systems with different boundary conditions [20,21]. It is believed that the continuous nanoparticle blades with higher thermal conductivity serve as the second conduction mechanism, and its optimized cooperation with the base fluid

of low thermal conductivity leads to the much better performance. In this study, the blade configuration of nanofluids is considered in detail by studying the influence of the shapes of high-conductivity blades in two kinds of building blocks of the total blade-configured heat conduction systems. This study is inspired by the need for the optimization of the cross section of duct for minimum flow resistance [11]. By treating heat as a flow medium flowing in blades, one can also find the optimal shape for the blades, which offers minimum thermal resistance.

Optimal blade shape for two kinds of building blocks of blade-configured heat conduction systems

The cylinder-shaped and regular-rectangular-prism-shaped building blocks are studied in this article. The nanoparticle blade has four different shapes: regular triangular prism, regular rectangular prism, regular hexagonal prism, and cylinder. For conciseness, the word "regular" is omitted hereafter. A format of "building-block-shape-blade-shape" is used to indicate the eight kinds of building blocks. Figure 1 shows the two kinds of building blocks with cylinder blades. For all the eight kinds of building blocks, uniform heat generation rate occurs in the base fluid region. All the external surfaces, except the cross-sectional plane $x = 0$ of the blade, are adiabatic. The cross-sectional plane $x = 0$ of the blade serves as the heat sink

* Correspondence: lqwang@hku.hk
Department of Mechanical Engineering, The University of Hong Kong, Pokfulam Road, Hong Kong



with constant temperature. The composition of these two-material building blocks is fixed by volume fraction

$$\phi = \frac{\text{volume of nanoparticle material}}{\text{total volume}}. \quad (1)$$

It is assumed that $\phi \ll 1$, and the thermal conductivity ratio of nanoparticle material and base fluid material is fixed and large. The thermal contact resistance is not considered.

In order to study the influence of the blade shape, the materials of the base fluid and nanoparticle, volumetric heat generation rate, and volumes of the eight kinds of building blocks are also fixed, besides the volume fraction and thermal conductivity ratio; however, the slenderness is free to vary to achieve the constructal system (building block) overall temperature difference. Here, the slenderness refers to the ratio of the radius to length for the cylinder building block, and the ratio of the circumscribing cylinder radius to length for the rectangular prism building block. For the simplest cylinder-cylinder building block, analytical analysis can be made; the system overall temperature difference, the constructal system overall temperature difference, and the constructal slenderness can be obtained analytically. Based on a slenderness range predicted by the analytic result, the numerical calculation is then conducted for all the eight kinds of systems to obtain, as accurately as possible, the

results for comparison among different blade shapes and different building block shapes.

Analytical analysis for cylinder-cylinder building block

Owing to the much higher thermal conductivity of nanoparticle material, heat conduction inside this kind of building block can be considered to consist of two one-dimensional routes-radial conduction inside cross-sectional planes of the base fluid region and axial conduction along the blade.

For the radial heat conduction inside base fluid, the governing equation and boundary conditions are

$$k_f \frac{1}{r} \frac{d}{dr} \left(r \frac{dT}{dr} \right) + q''' = 0 \quad (2)$$

and

$$\begin{cases} r = r_0, & T = T_c \\ r = R_0, & \frac{dT}{dr} = 0 \end{cases}, \quad (3)$$

respectively, where, k_f is the thermal conductivity of the base fluid; q''' is the volumetric heat generation rate; T_c is the temperature at the interface of the blade and base fluid at $x = L_0$ (L_0 is the length of the building block); r_0 is the radius of the inner blade; and R_0 is the outer radius of the building block. By solving Equations

(2) and (3), the radial temperature distribution of the cross-sectional plane $x = L_0$ of the base fluid region is obtained:

$$T = \frac{q'''}{4k_f}(r_0^2 - r^2) + \frac{q'''R_0^2}{2k_f} \ln\left(\frac{r}{r_0}\right) + T_c. \quad (4)$$

For the axial conduction inside the blade, the governing equation and boundary conditions, respectively, are

$$\frac{d^2T}{dx^2} = -\frac{(R_0^2 - r_0^2)q'''}{k_p r_0^2} \quad (5)$$

and

$$\begin{cases} x = 0, & T = T_0 \\ x = L_0, & \frac{dT}{dx} = 0 \end{cases} \quad (6)$$

where k_p is the thermal conductivity of the nanoparticle material, and T_0 is the heat-sink temperature at the cross-sectional plane $x = 0$ of the blade. By solving Equations (5) and (6), the axial temperature distribution along the blade is obtained as

$$T = -\frac{q'''(R_0^2 - r_0^2)}{2k_p r_0^2} x^2 + \frac{q'''(R_0^2 - r_0^2)L_0}{k_p r_0^2} x + T_0. \quad (7)$$

Thus, the overall temperature difference of the building block is

$$T_{\max} - T_0 = \frac{q'''(r_0^2 - R_0^2)}{4k_f} + \frac{q'''R_0^2}{2k_f} \ln\left(\frac{R_0}{r_0}\right) + \frac{q'''(R_0^2 - r_0^2)L_0}{2k_p r_0^2}. \quad (8)$$

Nondimensionalizing this overall temperature difference with $\frac{q'''R_0^{4/3}L_0^{2/3}}{k_f}$ (constant), one has

$$\Delta\tilde{T}_{\max} = \frac{T_{\max} - T_0}{\frac{q'''R_0^{4/3}L_0^{2/3}}{k_f}} = \frac{r_0^2 - R_0^2}{4R_0^{4/3}L_0^{2/3}} + \frac{1}{2} \ln\left(\frac{R_0}{r_0}\right) + \frac{R_0^2 - r_0^2}{2k_f r_0^2} \left(\frac{L_0}{R_0}\right)^{4/3}, \quad (9)$$

Where $\Delta\tilde{T}_{\max}$ is the nondimensional system (building block) overall temperature difference, and $\tilde{k} = \frac{k_p}{k_f}$ is the ratio of the thermal conductivities of the nanoparticle material and the base fluid material. By substituting Equation (1) in Equation (9), $\Delta\tilde{T}_{\max}$ becomes

$$\Delta\tilde{T}_{\max} = \frac{\phi - 1 - \ln\phi}{4} \left(\frac{R_0}{L_0}\right)^{2/3} + \frac{1 - \phi}{2\tilde{k}\phi} \left(\frac{L_0}{R_0}\right)^{4/3}, \quad (10)$$

which indicates that the building block's overall temperature difference (or thermal resistance) depends on its slenderness $\frac{R_0}{L_0}$ under the same composing materials, composition ratio, volumetric heat generation rate, and total volume. Figure 2 typifies this dependence at

$\phi = 0.05$ and $\tilde{k} = 641.6667$ (thermal conductivity ratio of copper and water). By minimizing this nondimensional system overall temperature difference with respect to $\frac{R_0}{L_0}$, the nondimensional constructal system overall temperature difference can be obtained:

$$(\Delta\tilde{T}_{\max})_{\text{con}} = \frac{(T_{\max} - T_0)_{\text{con}}}{\frac{q'''R_0^{4/3}L_0^{2/3}}{k_f}} = \frac{3(1 - \phi)^{1/3}(\phi - 1 - \ln\phi)^{2/3}}{2 \cdot 4^{2/3}(\tilde{k}\phi)^{1/3}} \quad (11)$$

and

$$\left(\frac{R_0}{L_0}\right)_{\text{con}} = \sqrt{\frac{4(1 - \phi)}{\tilde{k}\phi(\phi - 1 - \ln\phi)}}. \quad (12)$$

At $\left(\frac{R_0}{L_0}\right)_{\text{con}}$, the best-performing cylinder-cylinder building block can be obtained. If one specifies $\phi = 0.05$ and $\tilde{k} = 641.6667$, then the optimal slenderness $\left(\frac{R_0}{L_0}\right)_{\text{con}}$ will be 0.240618, and the nondimensional constructal system overall temperature difference $(\Delta\tilde{T}_{\max})_{\text{con}}$ will be 0.296778, which is the lowest point in Figure 2. Similarly, for the other kinds of building blocks considered here, there also exists such a best-performing slenderness $\left(\frac{R_0}{L_0}\right)_{\text{con}}$.

Numerical calculation for all the eight kinds of building blocks

The actual heat conduction in the cylinder-cylinder building block is of course not a simple combination of two one-dimensional conductions. For the other kinds of building blocks, the flow of heat is even more complex. In order to have as accurately as possible results for the comparison, a finite volume computational fluid dynamics (CFD) code [22] is used for obtaining numerical results for all the eight kinds of building blocks.

The conservation of energy equations are

$$\frac{\partial^2 \tilde{T}}{\partial \tilde{x}^2} + \frac{\partial^2 \tilde{T}}{\partial \tilde{y}^2} + \frac{\partial^2 \tilde{T}}{\partial \tilde{z}^2} + c^2 \left(\frac{L_0}{R_0}\right)^{4/3} = 0 \quad (13)$$

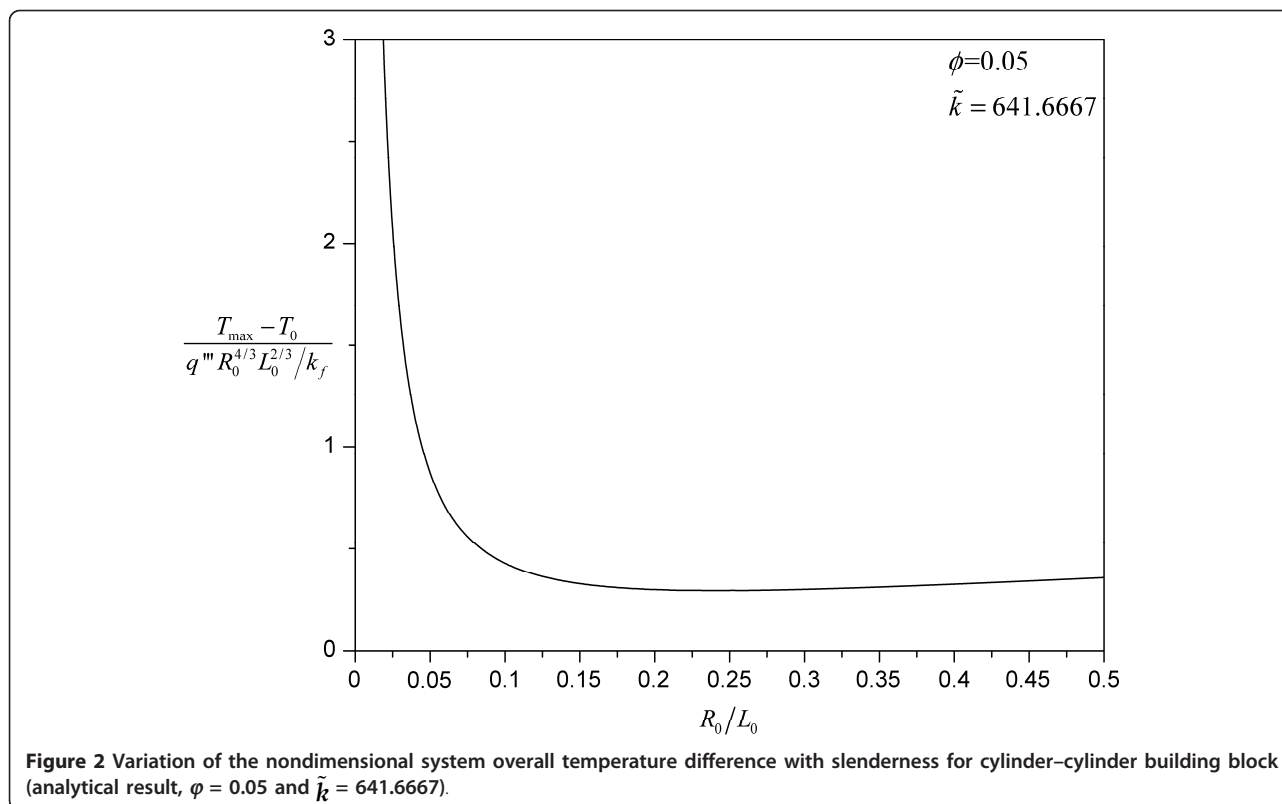
and

$$\frac{\partial^2 \tilde{T}}{\partial \tilde{x}^2} + \frac{\partial^2 \tilde{T}}{\partial \tilde{y}^2} + \frac{\partial^2 \tilde{T}}{\partial \tilde{z}^2} = 0 \quad (14)$$

for the base fluid and the blade, respectively. Here,

$$\tilde{T} = \frac{T - T_0}{\frac{q'''R_0^{4/3}L_0^{2/3}}{k_f}} + 1, \quad (\tilde{x}, \tilde{y}, \tilde{z}) = \frac{(x, y, z)}{cL_0}. \quad (15)$$

For rectangular-prism-series building blocks, R_0 stands for the radius of the circumscribing cylinder, for



which one has $R_0 = \frac{\sqrt{2}}{2}a$ (where a is the side length of the rectangular cross section). Constant, $c = 10 \cdot \frac{R_0}{L_0}$, is introduced to use fewer grids to achieve accurate enough results. The “+1” in the nondimensional temperature expression is introduced to ensure that the computing process does not touch the limit of 0 K. At the interface between the k_f region and k_p blade, the continuity of heat flux requires that

$$\left(\frac{\partial \tilde{T}}{\partial \tilde{\mathbf{n}}} \right)_f = \tilde{k} \left(\frac{\partial \tilde{T}}{\partial \tilde{\mathbf{n}}} \right)_p, \quad (16)$$

where $\tilde{\mathbf{n}}$ is the nondimensional normal vector; $\tilde{\mathbf{n}} = \frac{\mathbf{n}}{cL_0}$. As all the external surfaces, except the plane $x = 0$ of the k_p blade, are adiabatic,

$$\frac{\partial \tilde{T}}{\partial \tilde{\mathbf{n}}} = 0, \quad (17)$$

and for the plane $x = 0$ of the k_p blade, one has

$$\tilde{T} = 1. \quad (18)$$

Note that $(\tilde{T})_{\max} - 1$ is exactly the nondimensional system overall temperature difference, $\Delta \tilde{T}_{\max}$, as shown

in Equation (9), where $(\tilde{T})_{\max}$ is the maximal nondimensional temperature in the heat conduction building blocks.

It is specified that $\phi = 0.05$ and $\tilde{k} = 641.6667$ for the numerical calculation, the value used in the analytical analysis. The finite volume CFD code is chosen because of its efficiency and flexibility to generate a large number of results for various geometries which differ slightly from each other. Hexahedron grids are used to mesh the cylinder-hexagonal-prism and cylinder-cylinder building blocks, whereas all the other building blocks are meshed with wedge grids. Appropriate grid number is determined by doubling the interval number in \tilde{x} , \tilde{y} , and \tilde{z} directions each time, until the change of temperature becomes less than 0.05% (the maximal temperature, $(\tilde{T})_{\max}$, is used specifically for this criterion). Table 1 shows an example of how this grid independence is reached.

Table 1 Grid-independence check (cylinder-triangular-prism building block, $R_0/L_0 = 0.25$)

Number of grids	$(\tilde{T})_{\max} - 1$	Changing of $(\tilde{T})_{\max} - 1$
2500	0.271978	-0.010181×10^0
20120	0.269209	-8.803569×10^{-4}
167360	0.268972	-3.346073×10^{-5}
1248160	0.268963	

The nondimensional system overall temperature difference is shown in Figures 3 and 4 for the eight kinds of building blocks. The optimal slenderness $\left(\frac{R_0}{L_0}\right)_{\text{con}}$ and nondimensional constructal system overall temperature difference $(\Delta\tilde{T}_{\text{max}})_{\text{con}}$ for the cylinder–cylinder building block are 0.25 and 0.289577, respectively. Comparing with the approximate analytical results, the differences are only 3.75% and 2.49%, which confirms the accuracy of the finite volume CFD code.

All the eight kinds of heat conduction building blocks show strong performance dependence on the slenderness $\frac{R_0}{L_0}$ of the building blocks. Under the specific values for φ and \tilde{k} , the optimal slendernesses for the cylinder–series and rectangular-prism–series building blocks are 0.25 and 0.3, respectively, within a resolution of 0.05. Below the optimal slenderness, the performance dependence on $\frac{R_0}{L_0}$ increases in the order from cylinder–cylinder building block to cylinder–hexagonal-prism building block, cylinder–rectangular-prism building block, and then cylinder–triangular-prism building block. Above the optimal slenderness, this trend changes its direction. A similar situation happens for the rectangular-prism–series building blocks. When the $\frac{R_0}{L_0}$ value is small

enough ($\frac{R_0}{L_0} < 0.1$ for both the cylinder–series and rectangular-prism–series building blocks), the blade shape begins to have very weak effect on the system’s performance, due to the diminishing role played by the building block’s cross-sectional area when compared to its length. It can be seen from both Figures 3 and 4 that the four nondimensional system overall temperature difference curves almost collapse into one curve. For the cylinder–series building blocks, the collapsing curves approach the analytical result of the cylinder–cylinder building block as expected since the analytical result becomes more and more accurate as the $\frac{R_0}{L_0}$ value decreases. The analytical result shown in Figure 3 has the same φ and \tilde{k} values as those for the numerical calculation (the same curve as Figure 2). Thus, the accuracy of the finite volume CFD code is verified again. It should be noted that both the cylinder–series and rectangular-prism–series building blocks have fixed optimal slenderness. Therefore, the triangular-prism–shaped blade always performs the best among the four kinds of blades considered. Besides, the performance difference between successively shaped blades decreases from triangular-prism blade to cylinder blade, which is consistent with their surface area changing under the same volume, as shown in Table 2. Here, the surface area of

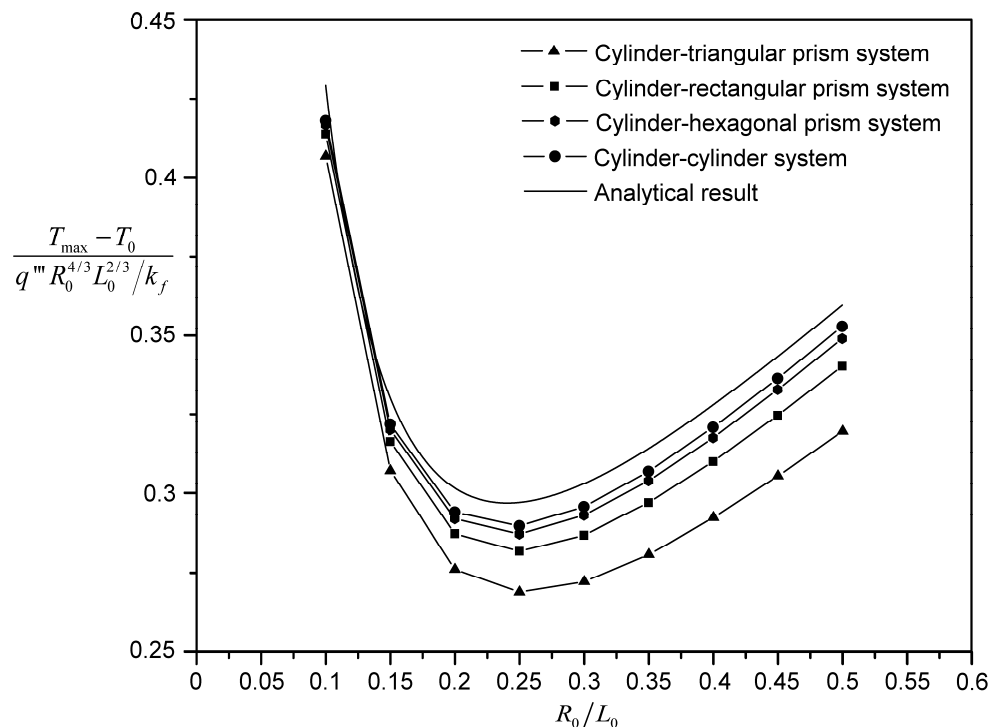


Figure 3 Numerical results for the cylinder–series building blocks and the analytical result for the cylinder–cylinder building block ($\varphi = 0.05$ and $\tilde{k} = 641.6667$).

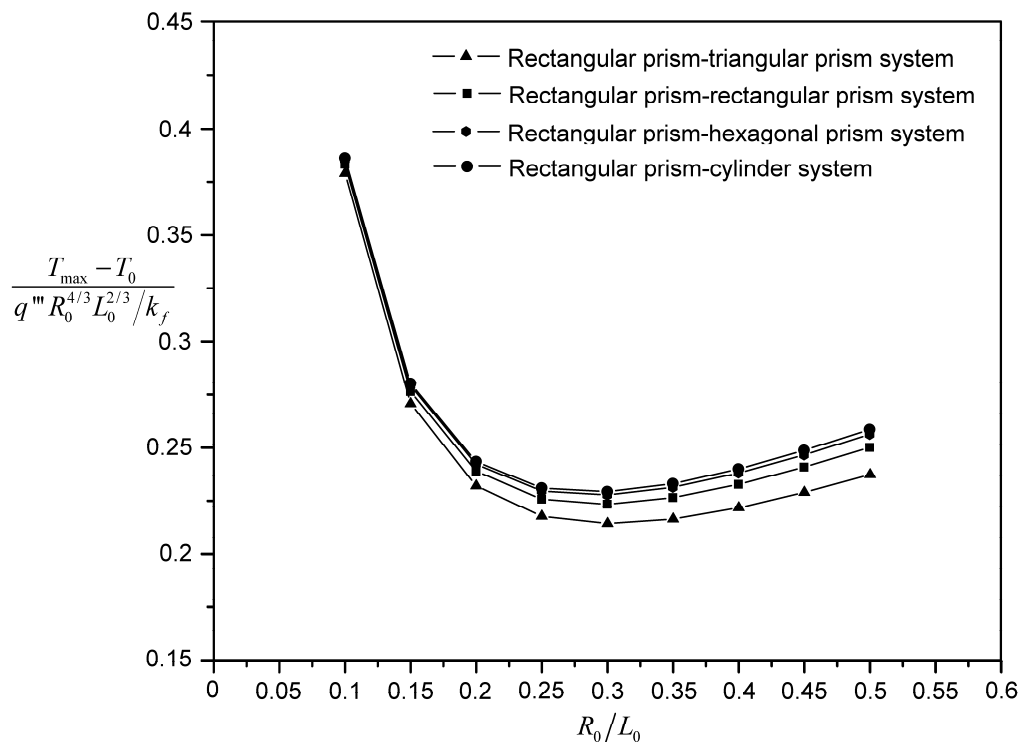


Figure 4 Numerical results for the rectangular-prism-series building blocks ($\phi = 0.05$ and $\tilde{k} = 641.6667$).

the blade is exactly the interfacial area between the base fluid and the blade. Thus, it is very likely that the performance difference can be attributed to the interfacial area difference: larger interfacial area will facilitate more low-temperature surfaces for the heat generation region, thereby lowering the maximal temperature in that region.

Therefore, under the same composing materials ($\tilde{k} = 641.6667$), composition ratio ($\phi = 0.05$), volumetric heat generation rate and total volume, the cylinder-triangular-prism and rectangular-prism-triangular-prism building blocks with slenderness values of 0.25 and 0.3, respectively, should be used for achieving the lowest system overall temperature difference (or, system thermal resistance) in practical applications. Both the pursuits of energy and material savings make this aim very significant. Furthermore, if one can also set the outer shape of

the heat conduction building block free (often constrained by efficient packing and manufacturing), a comparison can be made between the constructal (both the blade shape and slenderness having been optimized) cylinder-triangular-prism building block and constructal rectangular-prism-triangular-prism building block. Since the total volumes for the cylinder-series and rectangular-prism-series building blocks are $\pi R_0^2 L_0$ and $2R_0^2 L_0$, respectively, to ensure that the comparison is based on the same total building-block volume, the non-dimensional constructal system overall temperature difference of the cylinder-triangular-prism building block is divided by $\pi^{2/3}$

$$(\Delta \tilde{T}_{\max})_{\text{con,cyl}} = \frac{T_{\max} - T_0}{q''' \pi^{2/3} R_0^{4/3} L_0^{2/3} / k_f} = \frac{0.268972}{\pi^{2/3}} = 0.125393, \quad (19)$$

and the nondimensional constructal system overall temperature difference of the rectangular-prism-triangular-prism building block is divided by $2^{2/3}$

$$(\Delta \tilde{T}_{\max})_{\text{con,rec}} = \frac{T_{\max} - T_0}{q''' 2^{2/3} R_0^{4/3} L_0^{2/3} / k_f} = \frac{0.214368}{2^{2/3}} = 0.135043. \quad (20)$$

Thus, the constructal cylinder-shaped heat conduction building block performs better than the rectangular-prism-shaped building block.

Table 2 Perimeters of four blade cross sections having the same area of π

Cross section shape	Perimeter
Triangle	$3\sqrt{\frac{4\pi}{3}} = 8.080642$
Rectangle	$4\sqrt{\pi} = 7.089816$
Hexagon	$6\sqrt{\frac{2\pi}{3}} = 6.597817$
Circle	$2\pi = 6.283186$

Conclusions

Inspired by the duct cross section optimization for minimum flow resistance, the shape of the nanoparticle blade is optimized for the cylinder-shaped and rectangular-prism-shaped building blocks of the blade-configured heat conduction systems (blade configuration of nanofluids) based on the same composing materials, composition ratio, volumetric heat generation rate, and total building block volume. The four kinds of blade shapes are triangular prism, rectangular prism, hexagonal prism, and cylinder. For the cylinder-cylinder building block, analytical analysis can be conducted. Explicit expressions for the system overall temperature difference, constructal system overall temperature difference, and constructal slenderness can be obtained. Then, based on the slenderness range predicted by the analytical result, numerical calculations are performed for the eight kinds of building blocks to obtain as accurately as possible results for comparison. One specifies that $\phi = 0.05$ and $\tilde{k} = 641.6667$ for the numerical calculation.

The performances of the eight kinds of building blocks depend strongly on the building-block slenderness. The constructal slendernesses leading to minimum system overall temperature differences (system thermal resistances) are 0.25 and 0.3, respectively, for the cylinder-series and rectangular-prism-series building blocks. For both the cylinder-series and rectangular-prism-series building blocks, the triangular-prism-shaped blade performs the best among all the four kinds of blades considered. This is explained by the size of interfacial area sustained by the four kinds of blades with a fixed volume. Also, the constructal cylinder-triangular-prism building block is proved to perform better than the constructal rectangular-prism-triangular-prism building block at the same composing materials, composition ratio, volumetric heat generation rate and total building-block volume.

Abbreviations

CFD: computational fluid dynamics.

Acknowledgements

The financial support from the Research Grants Council of Hong Kong (GRF718009 and GRF717508) and the CRCG of the University of Hong Kong (Project 10400920) is gratefully acknowledged.

Authors' contributions

Both authors contributed equally.

Competing interests

The authors declare that they have no competing interests.

Received: 6 December 2010 Accepted: 21 March 2011

Published: 21 March 2011

References

1. Choi SUS: Nanofluids: from vision to reality through research. *J Heat Transfer* 2009, **131**:033106.

2. Wang LQ, Wei XH: Nanofluids: synthesis, heat conduction, and extension. *J Heat Transfer* 2009, **131**:033102.
3. Beck MP, Yuan YH, Warrier P, Teja AS: The thermal conductivity of aqueous nanofluids containing ceria nanoparticles. *J Appl Phys* 2010, **107**:066101.
4. Lee J, Gharagozloo PE, Kolade B, Eaton JK, Goodson KE: Nanofluid convection in microtubes. *J Heat Transfer* 2010, **132**:092401.
5. Sinha K, Kavlicoglu B, Liu YM, Gordaninejad F, Graeve A: A comparative study of thermal behavior of iron and copper nanofluids. *J Appl Phys* 2009, **106**:064307.
6. Evans W, Prasher R, Fish J, Meakin P, Phelan P, Keblinski P: Effect of aggregation and interfacial thermal resistance on thermal conductivity of nanocomposites and colloidal nanofluids. *Int J Heat Mass Transfer* 2008, **51**:1431-1438.
7. Jang SP, Choi SUS: Role of Brownian motion in the enhanced thermal conductivity of nanofluids. *Appl Phys Lett* 2004, **84**:4316-4318.
8. Özerinç S, Kakaç S, Yazıcıoğlu AG: Enhanced thermal conductivity of nanofluids: a state-of-the-art review. *Microfluid Nanofluid* 2010, **8**:145-170.
9. Buongiorno J, Venerus DC, Prabhat N, McKrell T, Townsend J, Christianson R, Tolmachev YV, Keblinski P, Hu LW, Alvarado JL, Bang IC, Bishnoi SW, Bonetti M, Botz F, Cecere A, Chang Y, Chen G, Chen HS, Chung SJ, Chyu MK, Das SK, Di Paola R, Ding YL, Dubois F, Dzido G, Eapen J, Escher W, Funfschilling D, Galand Q, Gao JW, Gharagozloo PE, Goodson KE, Gutierrez JG, Hong HP, Horton M, Hwang KS, Iorio CS, Jang SP, Jarzebski AB, Jiang YR, Jin LW, Kabelac S, Kamath A, Kedzierski MA, Kieng LG, Kim C, Kim JH, Kim S, Lee SH, Leong KC, Manna I, Michel B, Ni R, Patel HE, Philip J, Poulikakos D, Reynaud C, Savino R, Singh PK, Song PX, Sundararajan T, Timofeeva E, Tirtak T, Turanov AN, Van Vaerenbergh S, Wen DS, Witharana S, Yang C, Yeh WH, Zhao WH, Zhou SQ: A benchmark study on the thermal conductivity of nanofluids. *J Appl Phys* 2009, **106**:094312.
10. Teja AS, Beck MP, Yuan YH, Warrier P: The limiting behavior of the thermal conductivity of nanoparticles and nanofluids. *J Appl Phys* 2010, **107**:114319.
11. Bejan A: *Shape and Structure, From Engineering to Nature* Cambridge: Cambridge University Press; 2000.
12. Bejan A, Lorente S: *Design with Constructal Theory* Hoboken: Wiley; 2008.
13. Bejan A, Lorente S, Lee J: Unifying constructal theory of tree roots, canopies and forests. *J Theor Biol* 2008, **254**:529-540.
14. Bejan A, Lorente S: The constructal law and the thermodynamics of flow systems with configuration. *Int J Heat Mass Transfer* 2004, **47**:3203-3214.
15. Bejan A, Lorente S: Constructal theory of generation of configuration in nature and engineering. *J Appl Phys* 2006, **100**:041301.
16. Reis AH: Constructal theory: from engineering to physics, and how flow systems develop shape and structure. *Appl Mech Rev* 2006, **59**:269-282.
17. Rocha LAO, Lorente S, Bejan A: Constructal design for cooling a disc-shaped area by conduction. *Int J Heat Mass Transfer* 2002, **45**:1643-1652.
18. Bejan A, Lorente S: The constructal law of design and evolution in nature. *Philos Trans R Soc B* 2010, **365**:1335-1347.
19. Chodak I, Krupa I: "Percolation effect" and mechanical behavior of carbon black filled polyethylene. *J Mater Sci Lett* 1999, **18**:1457-1459.
20. Bai C, Wang LQ: Constructal allocation of nanoparticles in nanofluids. *J Heat Transfer* 2010, **132**:052404.
21. Bai C, Wang LQ: Constructal structure of nanofluids. *J Appl Phys* 2010, **108**:074317.
22. FLUENT 6.3 Documentation, Fluent Inc. .

doi:10.1186/1556-276X-6-240

Cite this article as: Bai and Wang: Constructal blade shape in nanofluids. *Nanoscale Research Letters* 2011 **6**:240.